Biochemical and Biophysical Research Communications 445 (2014) 694–701

Contents lists available at ScienceDirect

Biochemical and Biophysical Research Communications

journal homepage: www.elsevier.com/locate/ybbrc

In-depth proteomic analyses of ovarian cancer cell line exosomes reveals differential enrichment of functional categories compared to the NCI 60 proteome

Ankit Sinha [a,b], Vladimir Ignatchenko [b], Alex Ignatchenko [b], Salvador Mejia-Guerrero [b], Thomas Kislinger [a,b,*]

[a] University of Toronto, Department of Medical Biophysics, Toronto, Ontario, Canada
[b] Princess Margaret Cancer Center, Toronto, Ontario, Canada

ARTICLE INFO

Article history:
Available online 14 January 2014

Keywords:
Epithelial ovarian cancer
Exosomes
Mass spectrometry
Proteomics
Trifluoroethanol

ABSTRACT

Molecular communication between cancer cells and its stromal microenvironment is a key factor for cancer progression. Alongside classic secretory pathways, it has recently been proposed that small membranous vesicles are alternative mediators of intercellular communication. Exosomes carry an effector-rich proteome with the ability to modulate various functional properties of the recipient cell. In this study, exosomes isolated from four epithelial ovarian cancer cell lines (OVCAR3, OVCAR433, OVCAR5 and SKOV3) were characterized using mass spectrometry-based proteomics. Using an optimized workflow consisting of efficient exosome solubilization and the latest generation of proteomic instrumentation, we demonstrate improved detection depth. Systematic comparison of our cancer cell line exosome proteome against public data (Exocarta) and the recently published NCI 60 proteome revealed enrichment of functional categories related to signaling biology and biomarker discovery.

1. Introduction

Epithelial neoplastic cells transition into a mesenchymal phenotype with increased motility and invasion, two fundamental hallmarks of cancer [1,2]. These changes in phenotype allow epithelial ovarian carcinoma (EOC) cells to adhere to mesothelial cells as part of the invasion process into the peritoneal cavity. Malignant invasion of the peritoneal cavity often results in the accumulation of ascitic fluid, which can be due to obstruction of lymphatic drainage or through non-obstructive mechanisms in which EOC cells secrete biomolecular factors to propagate a cancer supporting niche [1]. This is evident through analysis of ovarian cancer ascites, containing a multitude of cancer specific/promoting factors [3]. Hence, the interplay between neoplastic cells and its stroma is one of the key factors in cancer growth and progression [4,5]. Previous studies have shown that tumour cells can modulate their microenvironment by secreting biomolecular factors to promote angiogenesis, invasion and immunosuppression [6]. Recent studies have shown that such communication is not limited to classically secreted factors, but can also be mediated by various small extracellular vesicles, such as exosomes, which will be the primary focus of the current study. [7,8]. Exosomes are small (40–100 nm diameter) membranous vesicles secreted through the endocytic pathway by most cell types and tumour cells. The protein content and the biological role of exosomes are dependent on the secreting cell type. For instance, exosomes derived from dendritic cells support the survival of naïve T-cells [9], whereas exosomes derived from cancer cells promote angiogenesis, stromal remodeling and transfer of growth factors and receptors to modulate signaling pathways of fibroblasts and other stromal components [10,11]. This suggests that exosomes originating from cancer cells play a role in cancer progression and modulation of the tumor microenvironment and in-depth characterization of the protein cargo of exosomes will help to elucidate their precise biological function. Hence, we hypothesize that systematic analyses of the EOC exosome proteome and integration with available data resources will reveal enriched proteins and pathways, potentially involved in intercellular communication.

2. Materials and methods

2.1. Cell culture

The four EOC cell lines, OVCAR3, OVCAR433, OVCAR5 and SKOV3 cell lines were grown in RPMI-1640 media supplemented with 10% fetal bovine serum, and 100 U/ml penicillin–streptomycin (all from

* Corresponding author at: Princess Margaret Cancer Center, University Health Network, 101 College Street, TMDT 9-807, Toronto, Ontario, Canada.
E-mail address: thomas.kislinger@utoronto.ca (T. Kislinger).

0006-291X/$ - see front matter © 2014 Elsevier Inc. All rights reserved.
http://dx.doi.org/10.1016/j.bbrc.2013.12.070

Gibco, Canada). Cells were cultured in ten 150 mm dishes at 37 °C in a 5% CO_2 humidified incubator. Once 80% confluency was achieved, the supernatant was removed and the monolayer was rinsed twice with warm PBS followed by addition of 20 mL of serum free media (RPMI-1640 media without phenol red and 100 U/ml penicillin–streptomycin) per plate. Cells were starved for 48 h at 37 °C in a 5% CO_2 humidified incubator. The supernatant from each plate was collected and pooled into 50 mL conical tubes (for a total of 200 mL of supernatant from each cell line).

2.2. Exosome isolation

Total supernatant was subjected to differential centrifugation for exosome isolation as previously described [12]. All centrifugations were performed at 4 °C. Briefly, loose cells were pelleted at 300×*g* for 10 min, while cellular debris were pelleted at 2000×*g* for 20 min. The supernatant was recovered and microvesicles and small cellular artifacts were sedimented by centrifuging at 10,000×*g* for 30 min. The supernatant was concentrated from a total volume of 200 to 9 mL using a 3000 Da molecular weight cut-off centrifugal filter (Millipore, Germany). The concentrated suspension and was centrifuged in a Type 70.1 Ti ultracentrifuge rotor at 120,000×*g* for 2 h. The supernatant was gently removed and the exosome pellet and washed with 9 mL of PBS solution. A second round of ultracentrifugation was performed with the same parameters, yielding an enriched exosome pellet.

2.3. Transmission electron microscopy – TEM

Exosome pellets prepared as previously described were re-suspended in 20 μL of PBS buffer. Fixation, embedding and image acquisition by TEM was performed at the Advanced Bioimaging Centre, Department of Pathology & Laboratory Medicine at Mount Sinai Hospital, Toronto, Canada.

2.4. 2,2,2-Trifluoroethanol-assisted protein extraction and trypsin digestion

Exosome pellets were subjected to denaturation, reduction, alkylation and trypsinization with slight modifications as previously described [13,14]. Briefly, exosome pellets were re-constituted in 150 μL of 50% (v/v) 2,2,2-trifluoroethanol (TFE) in PBS buffer. The suspension was incubated at 60 °C for two hours with brief agitation every 30 min. Proteins were reduced with 5 mM of DTT (Sigma, Canada) at 60 °C for 30 min. Carbamidomethylation of reduced cysteines was performed with 25 mM of IAA (Sigma) for 30 min at room temperature in the dark. Subsequently, samples were diluted five times using freshly prepared 100 mM ammonium bicarbonate buffer at pH 8.0. Proteins were digested using 5 μg of mass spectrometry grade trypsin (Promega, USA) at 37 °C overnight. Digested peptide mixtures were desalted and purified using OMIX C18 pipette tips (Agilent, USA) and concentrated by vacuum centrifugation. The semi-dry pellet of peptides was reconstituted to a volume of 16 μL using LC–MS grade water/0.1% formic acid.

2.5. Mass spectrometry analysis

Peptide concentrations were determined using a NanoDrop spectrophotometer (Thermo Scientific). Mass spectrometry was carried out using a QExactive tandem mass spectrometer (Thermo Scientific) equipped with an Easy-Spray nano-electrospray ionization source (Thermo Scientific) coupled to an EASY-nLC 1000 nano flow ultra-performance liquid chromatography system (Thermo Scientific). Analytical chromatography was performed using a 50 cm EASY-Spray column (PepMap C18, 2 μm particles, 100 Å pore size; Thermo Scientific) heated to 40 °C. For each analysis 2 μg of peptides were loaded on the analytical column. Elution buffers used for reverse phase chromatography consisted of 0.1% (v/v) formic acid as solvent A and 100% acetonitrile with 0.1% (v/v) formic acid as solvent B. Peptides were separated over an analytical gradient of 5–30% solvent B in 230 min at a flow rate of 250 nL/minute. Data was acquired on a QExactive mass spectrometer running a top 10 data dependent acquisition method. All MS1 spectra were acquired at resolution of 70,000 with scan range of 400–1600 *m*/*z*, while MS/MS spectra were acquired at resolution of 17,500.

2.6. Database searching and protein identification

The acquired data was searched by MaxQuant version 1.4.1.2 [15] against the UniProt complete human proteome protein sequence database (version: 2012-07-19, number of sequences: 20,232). Searches were performed with fragment ion mass tolerance of 20 ppm, maximum missed cleavage of 2 and carbamidomethylation of cysteine was specified as a fixed modification and oxidation of methionine as variable modification. False discovery was controlled using a target/decoy approach with false discovery level set to 1% (for peptides and proteins). Only protein groups identified with at least two or more peptides (sum of razor and unique) were carried forward in the analysis.

2.7. Statistics and data analysis

All statistical analyses were performed using R and its standard packages. Gene Ontology and protein keyword analysis were performed using the Protein Center bioinformatics software (Thermo Scientific). Only enriched groups with FDR p-value < 0.05 were reported.

2.8. Comparison to Exocarta and the NCI 60 proteome

A list of the 25 most commonly reported gene products in exosome studies were obtained from Exocarta [16,17]. Briefly, gene identifiers from all human exosome studies in Exocarta with protein evidence were mapped to our proteomics data (via gene identifiers; this increased the total number of 3096 protein groups to 3252 gene identifiers for our exosome data). Abundance intensities of exosome proteins shared with Exocarta were mapped against protein groups uniquely identified in the present study. Similarly, iBAQ intensities were used for the comparison of protein groups identified in the NCI 60 dataset and the current EOC exosomes analyses [18,19]. The NCI 60 dataset was mapped to our exosome data via the Protein Center software. Protein groups were considered statistically significantly different if $p < 0.05$ (Wilcoxon signed-rank test with p-values adjusted for multiple comparisons using Benjamini & Hochberg method) and biologically significantly different if protein intensity was equal or greater than a factor of two. Based on these criteria, protein groups were divided into three groups: higher abundance in exosome, equal abundance, and lower abundance in exosome.

2.9. Western blot analysis

All cells were harvested upon completion of 48 h starvation in serum-free media. The cell monolayer was washed twice with ice-cold PBS and scraped and lysed immediately in the presence of lysis buffer (20 mM Tris–HCl, 150 mM NaCl, 1 mM EDTA, 0.5% Igepal, pH 7.5 supplemented with a protease inhibitor cocktail; Roche Diagnostics) maintained at 4 °C. Exosome suspensions were lysed similarly. Cellular debris was removed by centrifugation (14,000×*g*, 10 min at 4 °C) and protein amount was determined

using a Pierce BCA protein assay kit (Fisher Scientific). Denaturing SDS–Polyacrylamide gel electrophoresis was performed in 12% acrylamide gels using equivalent total protein (10 μg for three cell lines; with the exception of OVCAR433 exosomes, where 30 μg were used). Separated proteins were transferred onto polyvinylidene difluoride membranes through electroblotting. Western blots were performed using primary and secondary antibodies coupled to HRP, diluted according to the suppliers' recommendations. The antibodies used were anti-CD81 (Santa Cruz Biotechnology, Dallas, Texas, USA), anti-flotillin-1 (FLOT-1, BD Biosciences, Mississauga, Ontario, Canada), anti-VDAC1 (Sigma–Aldrich), anti-calreticulin (CALR, Sigma–Aldrich), rabbit anti-aconitase 2 (ACO2, Sigma–Aldrich), mouse anti-GAPDH (Santa Cruz Biotechnology), and mouse anti-β-Actin (ACTB, Sigma–Aldrich). All antibodies were raised in mouse, except VDAC1 and ACO2 that were raised in goat and rabbit, respectively. Signals were visualized using the SuperSignal West Pico and Femto maximum sensitivity substrates system (Thermo Scientific). Upon completion of protein immunoblot, membranes were stained with PageBlue protein staining substrate (Thermo Scientific) to verify equal loading.

3. Results

3.1. In-depth proteomics of EOC-derived exosomes

The workflow for isolation and proteomics analysis of exosomes is described in Fig. 1A. Here, we starved cells for 48 h in serum-free media, which was subsequently used as the source for exosome isolation. Through differential centrifugation, cellular debris and larger microvesicles were pelleted and discarded, and high-speed ultracentrifugation (120,000×g) was used for exosome isolation. Exosome pellets were extracted using an optimized 2,2,2-trifloroethanol solubilization/digestion protocol prior to LC–MS analyses. Key to this project was the use of the latest generation of proteomics instrumentation utilizing a heated nano-flow ultra-high-performance liquid chromatography (UPLC) column coupled to a QExactive tandem mass spectrometer. Using rigorous peptide and protein identification criteria (MaxQuant; 1% FDR setting) a total of 3096 proteins groups were identified in exosomes obtained from four different EOC cell lines. Each was analyzed at two different passages as biological replicates

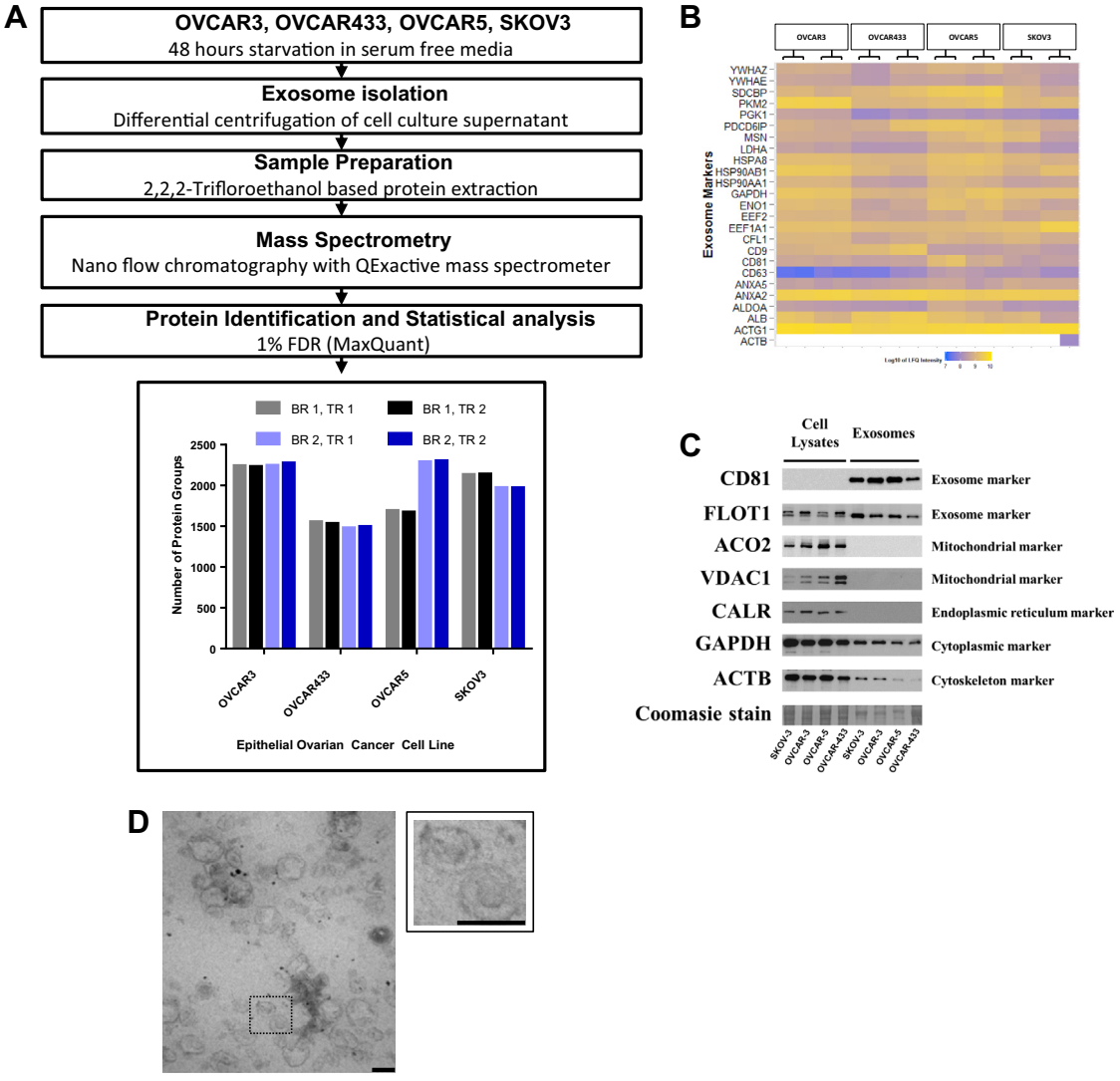

Fig. 1. Exosome isolation and analysis. (A) Reproducible numbers of protein groups were identified using the described workflow for each ovarian cancer cell line. (B) Proteomics analysis identified 24/25 commonly found exosomal proteins as reported by Exocarta. (C) Western blot analyses show increased intensities for exosomal markers (CD81, FLOT1) and lower intensities for negative control markers (VDAC1, CALR, ACO2, GAPDH and ACTB). (D) Representative transmission electron microscopy (TEM) images obtained for exosomes from OVCAR5. Scale bar: 100 nm.

(BR) and two technical replicates (TR) were performed (Suppl. Table 1).

Exocarta, a repository for exosome proteins, RNA and lipids, has aggregated 134 exosome studies to generate a list of 25 proteins with the highest frequency of identification in exosome studies [20]. The protein content identified in the 16 exosome analyses contained 24 of the top 25 commonly reported proteins in Exocarta (Fig. 1B). Detection of all marker proteins (except β-Actin; ACTB) in each analysis is indicative of high specificity of our proteomics data.

Western blot signal intensities for exosome markers such as CD81 and FLOT-1 were greater in the exosome fraction compared to the cell lysates (Fig. 1C). In conjunction, mitochondrial (ACO2 and VDAC1), endoplasmic reticulum (CALR) and cytoplasmic (GAPDH and ACTB) markers presented greater signal in cell lysate fractions than in exosomes. Changes in signal intensity in the western blot analyses (Fig. 1C) correlated well with trends in protein intensities reported by mass spectrometry (Fig. 1B). Firstly, SKOV3 had the largest ACTB western-blot signal intensity in the four exosome fractions, and similarly, ACTB was exclusively identified in SKOV3 exosome by mass spectrometry. Lastly, both exosome markers yielded the lowest signal in OVCAR433 exosomes compared to the other cell lines (Fig. 1C).

In addition to western blotting, we used TEM (Fig. 1D) to verify our exosome enrichment procedure. The majority of the detected vesicles range between the size of 40–100 nm, confirming effective enrichment of exosomes from the conditioned media [21].

3.2. Proteomic analyses showed high reproducibility

To assess the reproducibility of our chromatographic analyses, we performed ANOVA comparison of the elution time for nine base peaks (spread throughout the gradient, 15–248 min) in the two TR and two BR of OVCAR3 exosomes. The comparison did not show statistically significant differences ($p = 0.9338$, Fig. 2A) in elution

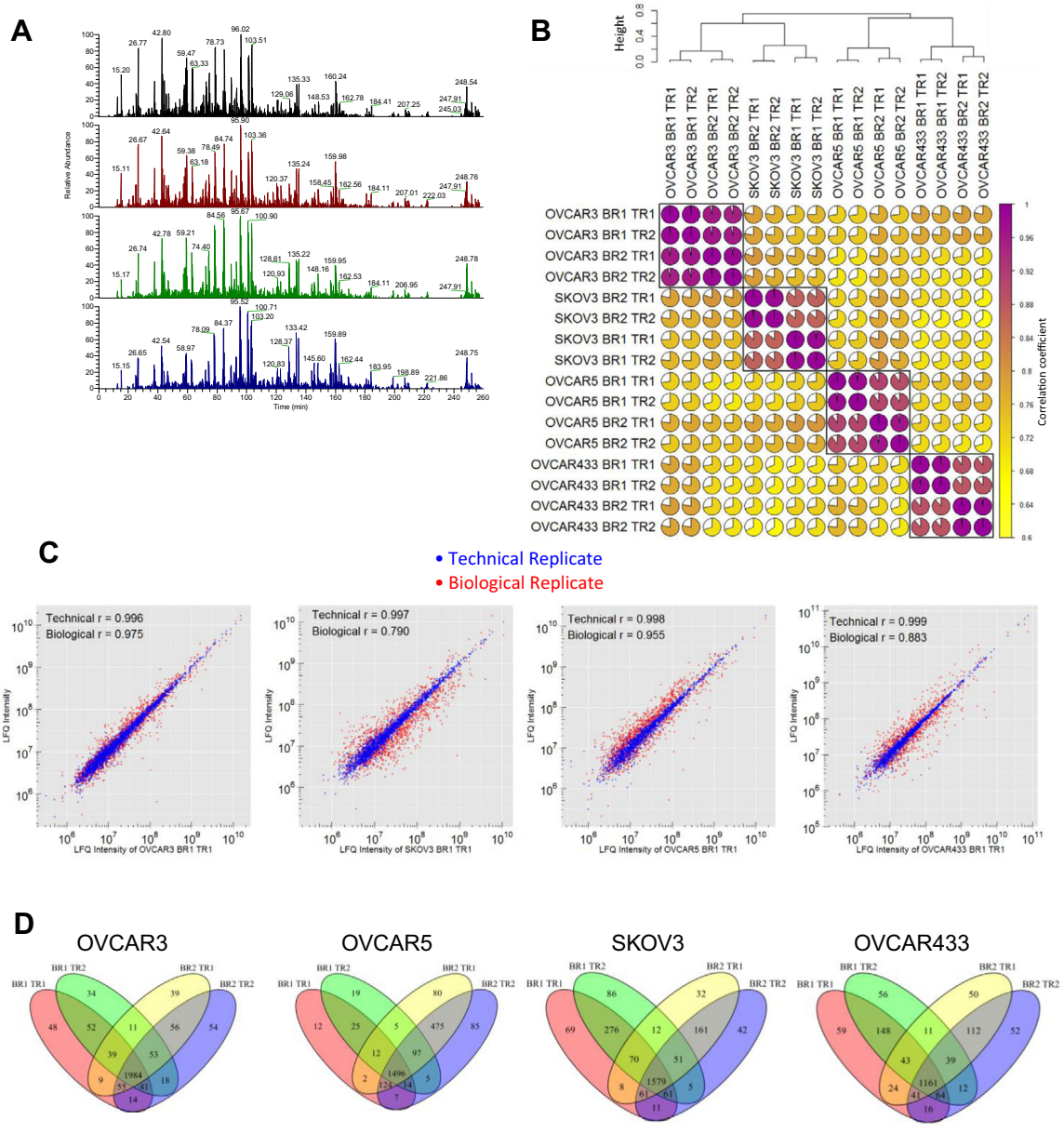

Fig. 2. Technical overview of the exosome proteomics data. (A) Total ion currents for the four OVCAR3 runs show high degree of chromatographic and mass spectrometry precision. (B) Correlation plot of LFQ protein intensities show the highest correlation between technical replicates, followed by biological replicated and the lowest correlation among different cell lines. (C) Scatter plots show high reproducibility among protein intensities between individual runs for each of the analyzed cell lines. (D) Venn diagrams show high reproducibility for protein identification among individual analyses. BR = biological replicate; TR = technical replicate.

time observed in the four runs, suggesting high reproducibility. Unsupervised clustering of all 16 analyses showed the highest correlation between technical replicates ($r > 0.9$), followed by biological replicates ($0.9 > r > 0.8$) and the lowest correlation between exosomes from different EOC cell lines ($0.8 > r > 0.6$; Fig. 2B). Similarly, the even distribution of scatter points along unity suggests absence of systematic bias in protein intensities between technical and biological replicates and a measurement range of 5.5 orders of magnitude (Fig. 2C). As expected, scatter points are more dispersed in biological replicates than technical replicates and the dispersion of intensity is greater for lower intensity protein groups. Random sampling effects are near minimal as protein groups uniquely identified to a single analysis only account for 3% of the total identifications (Fig. 2D).

3.3. Integrative analyses and comparison to the Exocarta database

Protein keyword enrichment performed for the exosome data showed the greatest enrichment in keywords associated with post-translationally modified proteins such as acetylation and phosphorylation ($p < 0.001$, Fig. 3A). To further analyze this observation, we sub-divided the keyword phospho-protein into the sub-terms phospho-tyrosine and phospho-serine/threonine (of note, the current study did not identify phosphorylation sites, but rather proteins that have been previously reported as post-translationally modified). Within the keyword phospho-tyrosine, 22 proteins were linked to the PI3K-AKT signaling pathway. With respect to serine and threonine kinases, the phosphatidylinositol-3-kinase (PI3K), mitogen-activated protein kinase (MAPK), and

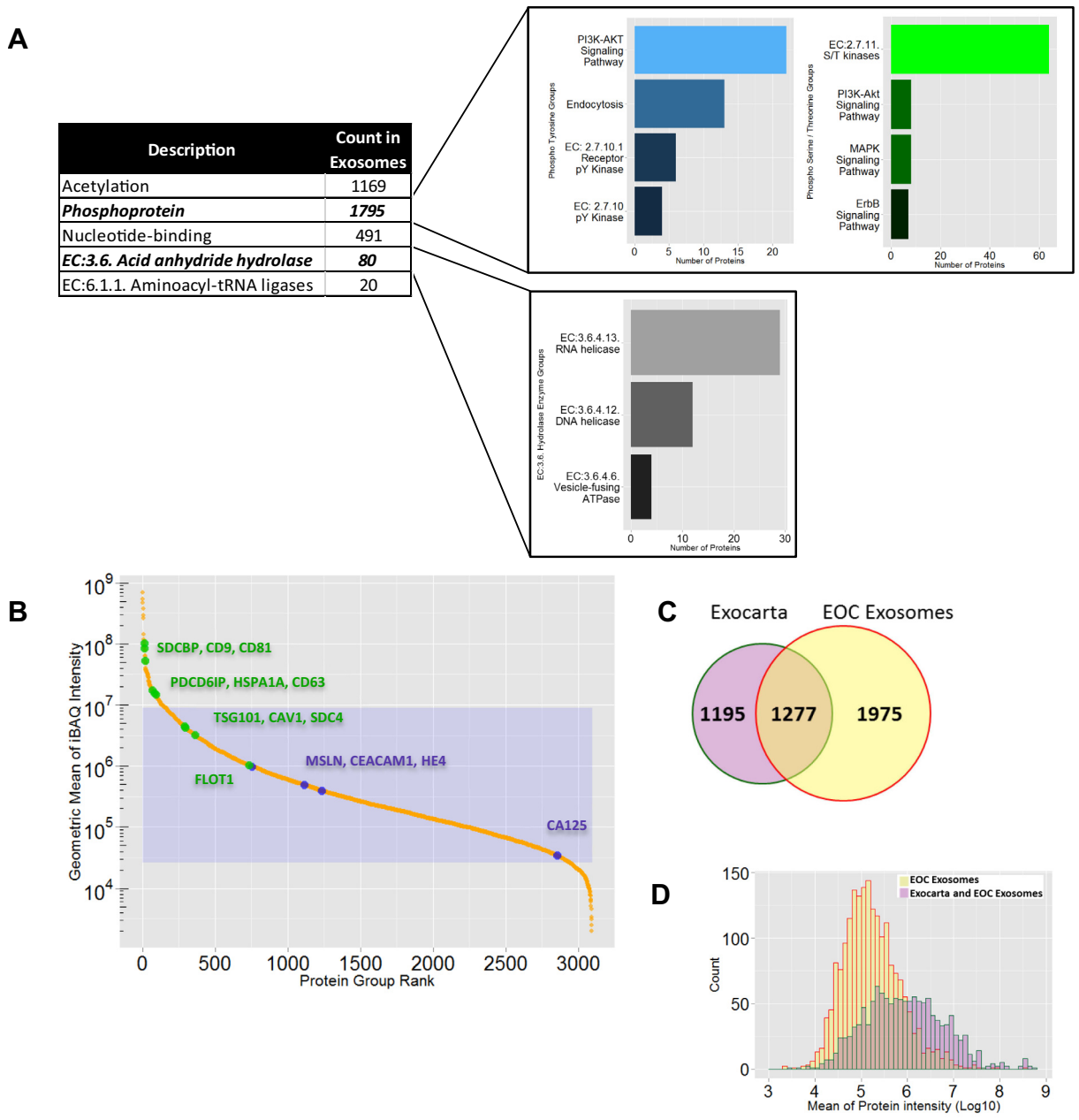

Fig. 3. Integrated analyses of the exosome proteome. (A) Selected examples of enriched keywords within the EOC exosome proteome revealed enrichment for various signaling pathways and proteins involved in vesicle fusion. (B) iBAQ protein intensities span six orders of magnitude with 90% of the proteome expressed within a narrow concentration range (shaded box). Commonly used exosome markers (green) are expressed more abundantly. In contrast, tumour markers (blue) such as CA125 and MSLN are less abundant. (C) Comparison of genes products in Exocarta and the current EOC exosome proteome. (D) Intensity histogram of protein groups identified unique to the EOC exosome proteome or in common with Exocarta revealed differences in protein abundance.

ErbB pathways were the most significantly enriched among the identified proteins. The most abundant protein function (based on keywords) was nucleotide binding, which supports the theory of the involvement of exosomes in manipulation of host cells [22]. Analysis for protein family domains yielded identification of 121 phospho-tyrosine kinases (PTKs, $p < 0.001$).

The intensity of identified protein groups in exosomes span 5.5 orders of magnitude, however 90% of the exosomal proteome was identified within 2.5 orders of magnitude, which also contains the common marker for EOC, CA125 (Fig. 3B). Commonly used exosome markers (marked in green) were in general of higher abundance. Comparison to proteins reported by the Exocarta database (i.e., protein level evidence was required) against our current EOC exosome proteome through gene level comparison (see Section 2), identified 1975 unique gene products not present in Exocarta and 1277 overlapping gene products (Fig. 3C). By binning the different protein groups identified in the two fractions (i.e., unique to current study or overlapping with Exocarta) according to protein intensity, it became evident that the protein groups identified exclusively in this study are of lower abundance (Fig. 3D), suggesting increased sensitivity of our current study. This is likely due to better chromatography and mass spectrometry instrumentations available in the current study.

3.4. Systematic comparison to the NCI 60 proteome

Lastly, we compared the recently published near complete proteome of the NCI 60 cell lines against our EOC exosome proteome.

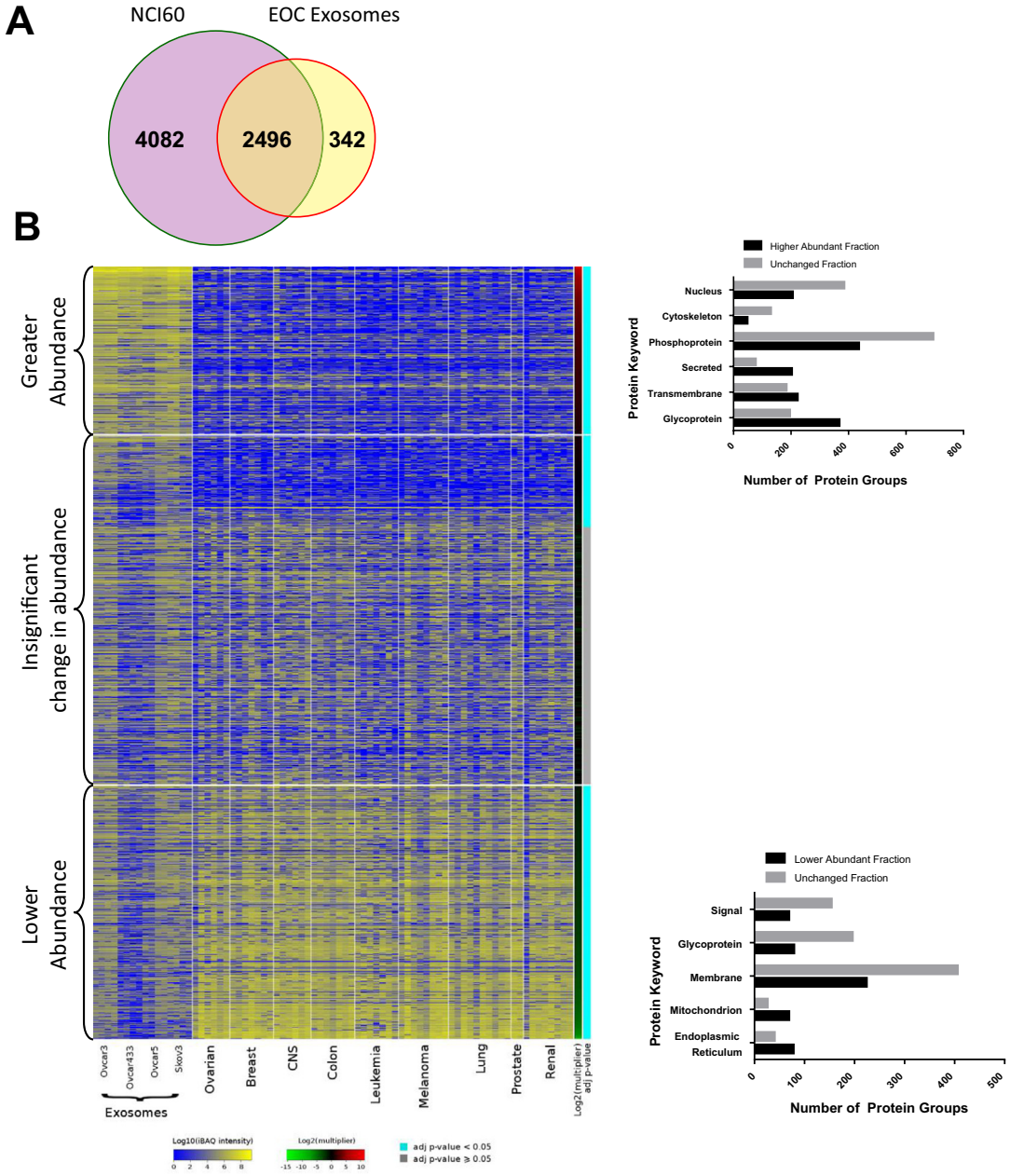

Fig. 4. Comparative analysis against the NCI 60 proteome. (A). Comparison of the NCI 60 cell line proteome against the current EOC exosome proteome. (B). Heatmap of shared protein groups between the NCI 60 and EOC exosome proteomes revealed 585 protein groups with higher intensity in exosomes, 880 protein groups with lower intensity in exosomes and 1212 unchanged protein groups. Functional annotation revealed enrichment in keywords such as glycoprotein, transmembrane and secreted in the exosome enriched cluster, whereas intracellular keywords such as mitochondrion or endoplasmic reticulum were enriched in the exosome depleted cluster.

Comparing the protein groups present in the two datasets revealed 2496 protein groups identified in both datasets and 342 and 4082 protein groups unique to exosomes or the NCI 60 cell lines, respectively (Fig. 4A). For the shared protein groups, a comparison of iBAQ intensities revealed 585 protein groups with two fold increased intensity in the exosome proteome ($p < 0.05$, Fig. 4B). On the other hand, 862 protein groups had >2-fold reduced protein intensities in the exosome proteome ($p < 0.05$, Fig. 4B). The remaining protein groups were either statistically indifferent or had less than two fold change in protein intensity. Subsequently, we performed keyword analysis on 928 protein groups that were either more abundant or exclusively identified in exosomes. In this sub-set, the greatest numbers of proteins were annotated with the keywords glycoprotein or transmembrane domain. This cluster also has lower frequency of keywords associated with intracellular organelles (nucleus, cytoskeleton). Similar analysis of the exosome depleted protein cluster (i.e. lower abundance proteins) showed the opposite trend. This subgroup had the greatest occurrence of endoplasmic reticulum and mitochondrial keywords, while glycosylated and membrane keywords were of lower frequency.

4. Discussion

The objective of this study was to present an in-depth proteomic characterization of EOC exosomes using the latest generation of chromatographic and mass spectrometric instrumentation. Exosome isolation combined with high resolution chromatography and mass spectrometry will allow for more detailed interrogation of the exosome proteome potentially leading to a better understanding of their biological function. A crucial step of the current study was to utilize a TFE-based extraction of proteins from exosomes. It has been previously reported that this extraction of membrane proteins is comparable to urea-based or conventional detergent-based extraction methods [23]. However, TFE extraction allows for reduced amount of initial sample as organic solvents minimize sample loss through decreased requirements for cleanup and transfer steps [24]. We first verified the validity of our exosome enrichment method using western blotting, TEM and MS-based proteomics (Fig. 1B–D). In immunoblotting, increased signal intensity was observed for known exosome markers (CD81 and FLOT1), while mitochondrial, ER and cytoplasmic markers had greater signal intensity in the cell lysates. Proteomics analyses also confirmed the presence of 24 out of 25 exosome markers previously reported by Exocarta. Interestingly, significantly fewer protein groups were identified in the exosomes of the OVCAR433 cells (Fig. 1A) and a similar trend was observed by Western blotting, as nearly three times more protein amount had to be loaded to obtain a reproducible signal (Fig. 1C). The reason for this observation requires further investigation in the future.

Subsequently, we evaluated the technical and biological quality of the proteomics data. For each cell line, we performed two replicate biological analyses that differed in exosomes being collected from different passages, and each passage was analyzed twice. The base peak chromatograms show high precision in elution time as well as peak intensity. A key contributor to reproducible elution time and peak intensity is the use of heated nano-flow columns combined with the increased separation efficiency of ultra-performance liquid chromatography. Unsupervised clustering of the 16 analyses revealed high correlation between technical and biological replicates, and a linearity over 5.5 orders of magnitude (Fig. 2B and C). The lower correlation between different cell lines can be attributed to the heterogeneous genetic profile of EOC cell lines [25]. Our proteomics data also exhibited high technical reproducibility as evidenced by the low percentage of identification unique to a single run. Hence, the combination of reproducible proteomic analyses (LC–MS) and the high correlation of protein group intensities suggest an overall robust analysis platform.

To obtain a systematic insight into the EOC exosome proteome, we identified enriched Uniprot keywords for the 3096 protein groups. Phosphorylation was the most abundant keyword, highlighting the potential involvement of exosome cargo in modulating signaling pathways. Phospho-tyrosine kinases were enriched by PFAM domain analysis and by KEGG pathway analysis. We categorized kinases according to their respective signaling pathways (Fig. 3A). The three most enriched pathways were ErbB, PI3K and MAPK, all of which are involved in cancer progression and migration. Protein acetylation was the second most abundant keyword, as N-terminal acetylation increases protein stability and half-life [26].

Exosomes have also been described as a rich source for the discovery of tumour biomarkers. We initially ranked all identified protein groups based on iBAQ intensities, as shown in Fig. 3B, to illustrate the dynamic range of protein intensities within the exosome proteome [18]. However, protein intensities calculated from the sum of the three highest peptide intensities provided a more reliable estimate of dynamic range [27]. EOC relevant tumour markers such as MUC16, WFDC2, CEA and MSLN are ranked within 2.6 orders of magnitude, which contain 90% of the identified proteins. Since exosomes have a narrower protein abundance range (proteins in body fluids span up to ten orders of magnitude) and contain tumour markers, they represent an interesting source for the discovery of fluid-based tumour markers. To evaluate the coverage of the exosome proteome, we compared our data against Exocarta, which revealed 1975 gene products not previously reported to be associated with exosomes, and 1277 gene products overlapping in both data. By comparing the histogram of binned protein intensity for these two groups an increased detection of lower abundance proteins was observed in the current study (Fig. 3D).

Finally, with the aim to characterize protein cargo that is differentially present in exosomes compared to cellular lysates, we compared the exosome proteome against the recently published NCI 60 proteome. This comparison revealed 342 protein groups unique to the current study and 2496 protein groups shared between exosomes and NCI 60 cell lysates. We further stratified the common protein groups into three categories based on statistical significance and fold change. The subgroup containing proteins with higher intensity in exosomes than in the NCI 60 cell lysates showed enrichment for keywords related to membrane proteins (glycoprotein, transmembrane) or the extracellular space (secreted proteins). The less frequent protein keywords are nucleus and cytoplasmic, which correlated with the results obtained by western blotting (Fig. 1C). Similarly, the cluster of protein groups less abundant in exosomes consisted of keywords related to intracellular organelles (endoplasmic reticulum and mitochondria).

In conclusion, we report a workflow for in-depth analysis of the exosome proteome and show enrichment of various signaling pathways. The described strategy was sensitive enough to detect more than 3000 exosomal protein groups, presenting a foundation for future analysis of cancer exosomes. Future investigations will focus on the application of the current analysis pipeline for the characterization of exosomes derived from ascites of EOC patients.

Acknowledgments

This work was supported in part by grants from the Canadian Institute of Health Research (MOP-93772) to T.K. This research was funded in part by the Ontario Ministry of Health and Long Term Care. The views expressed do not necessarily reflect those of the OMOHLTC. T.K. is supported through the Canadian Research Chairs Program. A.S. is supported through a Medical Biophysics

Excellence Award and the Kristi Piia Callum Memorial Fellowship. We would like to thank Dr. Rottapel (Princess Margaret Cancer Center) for providing the EOC cell lines.

Appendix A. Supplementary data

The data have been deposited to the ProteomeXchange with identifier PXD000695. Supplementary data associated with this article can be found, in the online version, at http://dx.doi.org/10.1016/j.bbrc.2013.12.070.

References

[1] E. Kipps, D.S. Tan, S.B. Kaye, Meeting the challenge of ascites in ovarian cancer: new avenues for therapy and research, Nat. Rev. Cancer 13 (4) (2013) 273–282.
[2] D. Hanahan, R.A. Weinberg, Hallmarks of cancer: the next generation, Cell 144 (5) (2011) 646–674.
[3] S. Elschenbroich et al., In-depth proteomics of ovarian cancer ascites: combining shotgun proteomics and selected reaction monitoring mass spectrometry, J. Proteome Res. 10 (5) (2011) 2286–2299.
[4] T.D. Tlsty, L.M. Coussens, Tumor stroma and regulation of cancer development, Annu. Rev. Pathol. 1 (2006) 119–150.
[5] Y. Mao et al., Stromal cells in tumor microenvironment and breast cancer, Cancer Metastasis Rev. 32 (1–2) (2013) 303–315.
[6] S.S. McAllister et al., Systemic endocrine instigation of indolent tumor growth requires osteopontin, Cell 133 (6) (2008) 994–1005.
[7] J.A. Cho et al., Exosomes from ovarian cancer cells induce adipose tissue-derived mesenchymal stem cells to acquire the physical and functional characteristics of tumor-supporting myofibroblasts, Gynecol. Oncol. 123 (2) (2011) 379–386.
[8] S. Principe et al., Tumor-derived exosomes and microvesicles in head and neck cancer: implications for tumor biology and biomarker discovery, Proteomics 13 (10–11) (2013) 1608–1623.
[9] K. Matsumoto et al., Exosomes secreted from monocyte-derived dendritic cells support in vitro naive CD4+ T cell survival through NF-(kappa)B activation, Cell. Immunol. 231 (1–2) (2004) 20–29.
[10] M. Iero et al., Tumour-released exosomes and their implications in cancer immunity, Cell Death Differ. 15 (1) (2008) 80–88.
[11] H. Peinado et al., Melanoma exosomes educate bone marrow progenitor cells toward a pro-metastatic phenotype through MET, Nat. Med. 18 (6) (2012) 883–891.
[12] C. Thery et al., Isolation and characterization of exosomes from cell culture supernatants and biological fluids, Curr. Protoc. Cell Biol. (2006). Chapter 3: p. Unit 3 22.
[13] L. Canelle et al., A proteomic approach to investigate potential biomarkers directed against membrane-associated breast cancer proteins, Electrophoresis 27 (8) (2006) 1609–1616.
[14] J.M. Deshusses et al., Exploitation of specific properties of trifluoroethanol for extraction and separation of membrane proteins, Proteomics 3 (8) (2003) 1418–1424.
[15] J. Cox, M. Mann, MaxQuant enables high peptide identification rates, individualized p.p.b.-range mass accuracies and proteome-wide protein quantification, Nat. Biotechnol. 26 (12) (2008) 1367–1372.
[16] S. Mathivanan, R.J. Simpson, ExoCarta: a compendium of exosomal proteins and RNA, Proteomics 9 (21) (2009) 4997–5000.
[17] R.J. Simpson, H. Kalra, S. Mathivanan, ExoCarta as a resource for exosomal research, J. Extracellular Vesicles (2012) 1.
[18] L. Arike et al., Comparison and applications of label-free absolute proteome quantification methods on *Escherichia coli*, J. Proteomics 75 (17) (2012) 5437–5448.
[19] A. Moghaddas Gholami et al., Global proteome analysis of the NCI-60 cell line panel, Cell Rep. 4 (3) (2013) 609–620.
[20] S. Mathivanan et al., ExoCarta 2012: database of exosomal proteins, RNA and lipids, Nucleic Acids Res. 40 (Database issue) (2012) D1241–D1244.
[21] H. Kalra et al., Comparative proteomics evaluation of plasma exosome isolation techniques and assessment of the stability of exosomes in normal human blood plasma, Proteomics 13 (22) (2013) 3354–3364.
[22] H. Zhou et al., Urinary exosomal transcription factors, a new class of biomarkers for renal disease, Kidney Int. 74 (5) (2008) 613–621.
[23] H. Zhang et al., Differential recovery of membrane proteins after extraction by aqueous methanol and trifluoroethanol, Proteomics 7 (10) (2007) 1654–1663.
[24] H. Wang et al., Development and evaluation of a micro- and nanoscale proteomic sample preparation method, J. Proteome Res. 4 (6) (2005) 2397–2403.
[25] S. Domcke et al., Evaluating cell lines as tumour models by comparison of genomic profiles, Nat. Commun. 4 (2013) 2126.
[26] T. Arnesen, Towards a functional understanding of protein N-terminal acetylation, PLoS Biol. 9 (5) (2011) e1001074.
[27] E. Ahrne et al., Critical assessment of proteome-wide label-free absolute abundance estimation strategies, Proteomics 13 (17) (2013) 2567–2578.